Ultrasound directed self-assembly of user-specified patterns of nanoparticles dispersed in a fluid medium

J. Greenhall,[1] F. Guevara Vasquez,[2] and B. Raeymaekers[1,a)]
[1]Department of Mechanical Engineering, University of Utah, Salt Lake City, Utah 84112, USA
[2]Department of Mathematics, University of Utah, Salt Lake City, Utah 84112, USA

(Received 1 February 2016; accepted 27 February 2016; published online 9 March 2016)

We employ an ultrasound wave field generated by one or more ultrasound transducers to organize large quantities of nanoparticles dispersed in a fluid medium into two-dimensional user-specified patterns. To accomplish this, we theoretically derive a direct method of calculating the ultrasound transducer parameters required to assemble a user-specified pattern of nanoparticles. The computation relates the ultrasound wave field and the force acting on the nanoparticles to the ultrasound transducer parameters by solving a constrained optimization problem. We experimentally demonstrate this method for carbon nanoparticles in a water reservoir and observe good agreement between experiment and theory. This method works for any simply closed fluid reservoir geometry and any arrangement of ultrasound transducers, and it enables using ultrasound directed self-assembly as a scalable fabrication technique that may facilitate a myriad of engineering applications, including fabricating engineered materials with patterns of nanoscale inclusions. © *2016 AIP Publishing LLC*. [http://dx.doi.org/10.1063/1.4943634]

Directed self-assembly (DSA) is the process by which nanoparticles or other discrete components organize as a result of interactions between the components themselves and/or with their environment.[1] DSA relies on templated,[2,3] template-free,[4] and external field-directed techniques.[5–7] External field-directed techniques employ a set of transducers to generate an electric,[5] magnetic,[6] or ultrasound field[7] that acts as a tunable mask, and enables modifying a pattern of nanoparticles by adjusting the arrangement and operating parameters of the transducer(s). Electric and magnetic fields require using conductive and ferromagnetic nanoparticles, respectively, and demand an ultra-high field strength to organize nanoparticles into patterns,[8,9] thus limiting material choice and scalability. Ultrasound DSA relies on the acoustic radiation force associated with an ultrasound wave field to organize nanoparticles into user-specified patterns. In contrast with electric and magnetic fields, this technique works for particles with any material properties, and while this paper focuses on nanoparticles, it is applicable to any particle size that is significantly smaller than the wavelength of the ultrasound wave. Additionally, weak attenuation of ultrasound waves in most low-viscosity fluids reduces the need for ultra-high field strengths, thus facilitating scalability.[10] Hence, ultrasound DSA could enable fabricating complex multi-dimensional patterns of nanoparticles for use in a wide range of engineering applications, including biology,[11] biomedical devices,[12] process control,[13] and bottom-up manufacturing of engineered nanostructured materials whose exotic properties are derived from specific patterns of nanoparticles.[14–17] However, using ultrasound DSA as a fabrication technique requires relating the ultrasound transducer arrangement and parameters that generate the ultrasound wave field to the resulting pattern of nanoparticles that is assembled, as specified a priori by the pattern designer. This translates into two problems: (1) the "forward ultrasound DSA problem" entails calculating the pattern of nanoparticles resulting from user-specified ultrasound transducer parameters, and (2) the "inverse ultrasound DSA problem" involves calculating the ultrasound transducer parameters required to assemble a user-specified pattern of nanoparticles.

Solving the forward ultrasound DSA problem requires computing the acoustic radiation force associated with the ultrasound wave field generated by the ultrasound transducers. The resulting pattern of nanoparticles is then found as the stable fixed positions $\mathbf{x}_f$ of the acoustic radiation force, i.e., the location(s) where the force is zero and points toward $\mathbf{x}_f$ in the surrounding region.[18] The inverse ultrasound DSA problem is solved either directly or indirectly. Indirect methods solve the forward ultrasound DSA problem for a range of ultrasound transducer parameters and create a "map" that relates nanoparticle patterns to transducer parameters.[19–21] Direct methods have only been derived for a small number of specific reservoir and/or pattern geometries,[22–24] without providing a universal solution. Thus, the objective of this work is to demonstrate a direct solution methodology to the inverse ultrasound DSA problem for a user-specified pattern in any two-dimensional, simply closed reservoir geometry and ultrasound transducer arrangement.

We relate the user-specified pattern of nanoparticles to the ultrasound transducer parameters in two steps. First, we calculate the ultrasound wave field in an arbitrary shaped reservoir lined with ultrasound transducers around its perimeter as a function of the ultrasound transducer parameters using the boundary element method based on Green's third identity,[25] which relates the wave field within a simply closed domain to the boundary conditions imposed on the perimeter of that domain. Then, we calculate the acoustic radiation force acting on a spherical particle to determine the pattern of nanoparticles resulting from the ultrasound wave field.[18] Finally, we compute the ultrasound transducer parameters required to assemble a user-specified pattern of nanoparticles by solving a constrained nonconvex quadratic optimization problem using eigendecomposition. We present a theoretical

a)bart.raeymaekers@utah.edu

derivation and experimental validation. We clarify that this work is unrelated to ambisonics[26,27] and acoustic holography,[28] where a user-specified acoustic wave field, rather than the stable fixed points of the acoustic radiation force, is related to the ultrasound transducer parameters through unconstrained linear least squares optimization.

Figure 1 shows a two-dimensional arbitrary shaped reservoir filled with a fluid medium of density ρ_m and sound speed c_m, and lined with N_t ultrasound transducers of acoustic impedance Z_t around the perimeter. The inset of Fig. 1 illustrates the discretization of the domain perimeter S into $N_b \geq N_t$ boundary elements (black dots) and the domain D into N_d domain points (red dots), which may be selected in any arrangement. The j^{th} boundary element, identified by its center point $\mathbf{q}_j$, is $\varepsilon(\mathbf{q}_j)$ wide and is driven by the ultrasound transducer parameter $v(\mathbf{q}_j)$, i.e., the complex harmonic velocity (amplitude and phase) of the transducer surface along its normal direction $\mathbf{n}(\mathbf{q}_j)$, which acts as a piston source to create the ultrasound wave field. Additionally, we indicate a test point $\mathbf{x}_l$ in D with respect to the reservoir coordinates (x, y) with origin $\mathbf{o}$.

We use the boundary element method to calculate the ultrasound wave field with frequency ω_0 in terms of the time-independent, complex scalar velocity potential φ at each domain point within D. We note that: (1) φ must satisfy the Helmholtz equation $(\nabla^2\varphi + k_0^2\varphi = 0)$ in D, where $k_0 = \omega_0/c_m$ is the wave number of the ultrasound wave field in the fluid medium. (2) The impedance boundary condition $\partial\varphi/\partial\mathbf{n} + ik_0\tilde{Z}\varphi = v$ must be satisfied on S, where $\tilde{Z} = \rho_m c_m/Z_t$ is the impedance ratio, accounting for the absorption and reflection of the ultrasound wave within the fluid medium as it interacts with the ultrasound transducer surface. Arranging all ultrasound transducer parameters v into a vector $\mathbf{v}$, we calculate the ultrasound wave field at all N_d domain points as[25]

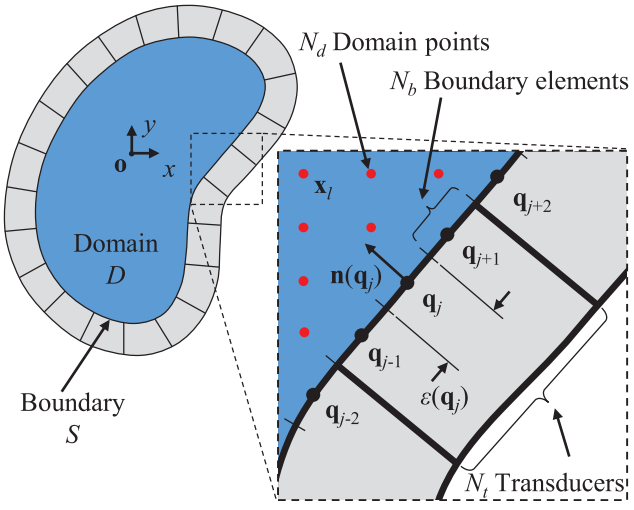

FIG. 1. Two-dimensional, arbitrary shaped fluid reservoir lined with N_t ultrasound transducers. The inset illustrates the discretization scheme of the boundary element method used to model the ultrasound directed self-assembly process, which divides the domain boundary into N_b boundary elements (black dots) and the domain into N_d domain points (red dots). Additionally, the inset shows the width $\varepsilon(\mathbf{q}_j)$ and normal direction $\mathbf{n}(\mathbf{q}_j)$ of the jth boundary element $\mathbf{q}_j$.

$$\boldsymbol{\varphi} = \mathbf{PWv}. \tag{1}$$

The matrix $\mathbf{W}$ maps each boundary element to its corresponding ultrasound transducer, i.e., $w_{jn} = 1$ if the j^{th} boundary element is contained within the n^{th} transducer, otherwise $w_{jn} = 0$. Additionally, each term p_{lj} of the matrix $\mathbf{P}$ corresponds to the ultrasound wave field created at $\mathbf{x}_l$ by a point source located at $\mathbf{q}_j$ on S, including all reflections from the reservoir walls. We calculate all p_{lj} terms in matrix form as

$$\mathbf{P} = \hat{\mathbf{B}} - \hat{\mathbf{A}}\left(\frac{1}{2}\mathbf{I} + \mathbf{A}\right)^{-1}\mathbf{B}. \tag{2}$$

$\mathbf{I}$ is the identity matrix and we compute each term a_{lj} and b_{lj} of the matrices $\mathbf{A}$ and $\mathbf{B}$ as

$$a_{lj} = \left[ik_0\tilde{Z}G(\mathbf{q}_j, \mathbf{x}_l) + \frac{\partial G(\mathbf{q}_j, \mathbf{x}_l)}{\partial \mathbf{n}(\mathbf{q}_j)}\right] \times \varepsilon(\mathbf{q}_j)\delta(\mathbf{q}_j, \mathbf{x}_l), \text{ and,} \tag{3}$$

$$b_{lj} = G(\mathbf{q}_j, \mathbf{x}_l)\varepsilon(\mathbf{q}_j)\delta(\mathbf{q}_j, \mathbf{x}_l). \tag{4}$$

Here, $i = \sqrt{-1}$, $\delta(\mathbf{q}_j, \mathbf{x}_l) = 0$ when $\mathbf{q}_j = \mathbf{x}_l$, otherwise, it is 1, and $G(\mathbf{q}_j, \mathbf{x}_l)$ is the Green's function, which represents the free-field ultrasound wave emitted from a point source located at $\mathbf{q}_j$ and measured at location $\mathbf{x}_l$, defined as[25]

$$G(\mathbf{q}_j, \mathbf{x}_l) = -\frac{i}{4}H_0\left(k_0|\mathbf{q}_j - \mathbf{x}_l|\right). \tag{5}$$

H_0 is the 0^{th} order Hankel function of the first kind, and $|\mathbf{q}_j - \mathbf{x}_l|$ is the distance between points $\mathbf{q}_j$ and $\mathbf{x}_l$. We obtain the matrices $\hat{\mathbf{A}}$ and $\hat{\mathbf{B}}$ in Eq. (2) analogously to $\mathbf{A}$ and $\mathbf{B}$, differing only by the selection of the points $\mathbf{x}_l$, which lay on S for $\mathbf{A}$ and $\mathbf{B}$, and lay in D for $\hat{\mathbf{A}}$ and $\hat{\mathbf{B}}$. Thus, using the boundary element method, we relate the ultrasound transducer parameters to the resulting ultrasound wave field.

To relate the ultrasound wave field to the pattern of nanoparticles, we calculate the acoustic radiation force acting on a nanoparticle of density ρ_p and sound speed c_p, dispersed in a fluid medium at location $\mathbf{x}_l$ in D as

$$\mathbf{f}_l = -\nabla U_l, \tag{6}$$

where U_l is the acoustic radiation potential at $\mathbf{x}_l$. For a spherical particle with radius $r_p \ll \lambda_0$, and $\lambda_0 = 2\pi c_m/\omega_0$, we find[18]

$$U_l = \mathbf{v}^H\mathbf{Q}_l\mathbf{v}, \tag{7}$$

where $\mathbf{v}^H$ is the conjugate transpose of $\mathbf{v}$, and the Hermitian matrix $\mathbf{Q}_l$ is calculated as

$$\mathbf{Q}_l = 2\pi r_p^3\rho_m\mathbf{W}^H\left\{\frac{1}{3}k_0^2\left[1 - \left(\frac{\beta_p}{\beta_m}\right)^2\right][\mathbf{p}_l\mathbf{p}_l^H] - \left[\frac{\rho_p - \rho_m}{2\rho_p + \rho_m}\right][(\nabla\mathbf{p}_l)(\nabla\mathbf{p}_l)^H]\right\}\mathbf{W}. \tag{8}$$

$\mathbf{p}_l^H$ is the l^{th} row of $\mathbf{P}$, and $\beta_m = 1/\rho_m c_m$ and $\beta_p = 1/\rho_p c_p$ are the compressibility of the fluid medium and particle, respectively. From Eq. (7), we calculate the obtained pattern

of nanoparticles as the region(s) consisting of points $\mathbf{x}_l$, where U_l is locally minimum. Thus, to achieve assembly of a user-specified pattern of nanoparticles consisting of the set of desired positions X_{des}, each value U_l corresponding to each position $\mathbf{x}_l \in X_{des}$, must be locally minimum with respect to the reservoir coordinates (x,y). We relax the requirement of local minimality to obtain an optimization problem with a single objective function by minimizing the average value of U_l for all points $\mathbf{x}_l \in X_{des}$, with respect to $\mathbf{v}$. We write this average as the quadratic function

$$\bar{U} = \mathbf{v}^H \bar{\mathbf{Q}} \mathbf{v}, \tag{9}$$

where the matrix $\bar{\mathbf{Q}}$ is the average of the matrices $\mathbf{Q}_l$ corresponding to each desired position $\mathbf{x}_l \in X_{des}$. $\bar{U}$ has no lower bound because $\bar{\mathbf{Q}}$ is indefinite. Physically, this means that particles assemble at the desired positions more effectively by increasing the harmonic velocity amplitude of the ultrasound transducer surfaces indefinitely ($|\mathbf{v}| \to \infty$). Practically, the function generator that energizes the ultrasound transducers limits the harmonic velocity amplitude of the transducer surfaces to finite values. Thus, we constrain the magnitude $|\mathbf{v}| = \alpha$, where α is a real, scalar value representing the maximum harmonic velocity of the ultrasound transducer surface that can be achieved with a function generator. Hence, we formulate the constrained quadratic optimization problem

$$\min \bar{U}, \text{ subject to } |\mathbf{v}| = \alpha. \tag{10}$$

From Eq. (10), we calculate the ultrasound transducer parameters $\mathbf{v}^*$ required to assemble a user-specified pattern of nanoparticles as the eigenvector corresponding to the smallest eigenvalue of $\bar{\mathbf{Q}}$, where $\mathbf{v}^*$ has length α.[29]

To demonstrate assembly of a complex user-specified pattern of nanoparticles, we define the University of Utah "U" logo within a square water reservoir with $N_t = 200$ transducers around the perimeter and compute the ultrasound transducer parameters $\mathbf{v}^*$ required to assemble this pattern using Eq. (10). Figure 2 shows the simulated pattern of nanoparticles resulting from the computed ultrasound transducer parameters $\mathbf{v}^*$ (black) and the corresponding acoustic radiation potential (green), together with the user-specified "U" pattern (red). We qualitatively observe a close match between the user-specified and simulated patterns, except at sharp edges of the pattern. When $\rho_p \neq \rho_m$ and $\beta_p \neq \beta_m$, the ultrasound DSA technique is limited to creating pattern features with finite curvature, and the minimum achievable pattern radius is inversely proportional to the frequency of the ultrasound wave. For instance, considering the concentric-circular pattern of a 0^{th} order Bessel function of the first kind, the maximum achievable curvature will coincide with the circle created at the smallest root of the Bessel function, with radius $R = 2.4048 \cdot c_m/\omega_0$. Extra features, not part of the user-specified pattern, may exist if the optimization (Eq. (10)) does not yield an exact match with the user-specified pattern for the specified ultrasound transducer arrangement, operating frequency ω_0, and reservoir geometry.

Figure 2 illustrates that this method enables creating complex patterns of nanoparticles. While the relationship between pattern complexity and the number of ultrasound transducers remains an open problem, it is evident that the ability to create a complex pattern of nanoparticles increases with increasing number of ultrasound transducers. Thus, to validate our model and method, we limit the experiments to $N_t = 4$ and 8 and focus on dot and line patterns of nanoparticles, which are commonly used in engineering applications.[11–13,15–17] Figure 3 shows a schematic of the experimental procedure. We define a user-specified pattern in a square reservoir filled with water and 80 nm carbon nanoparticles, lined with PZT transducers (type SM112) with center frequency $\omega_0/2\pi = 1.5$ MHz. The ultrasound transducer parameters $\mathbf{v}^* = [v_1, v_2, \ldots, v_{N_t}]^T$ obtained by solving Eq. (10) are applied to the N_t transducers using a function generator, and we record the assembled pattern of nanoparticles using a camera and compare it to the user-specified pattern.

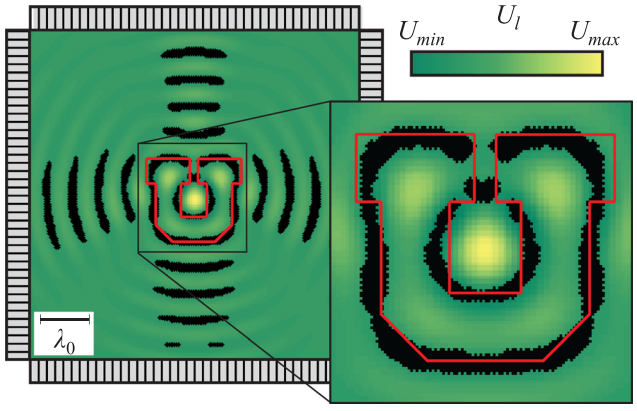

FIG. 2. Ultrasound directed self-assembly (DSA) of a University of Utah "U" pattern of nanoparticles. The ultrasound transducer parameters $\mathbf{v}^*$ required to assemble a user-specified "U" pattern (red) are calculated using the inverse ultrasound DSA method, and used to simulate a standing ultrasound wave with acoustic radiation potential U_l (green), which drives nanoparticles into the simulated "U" pattern (black).

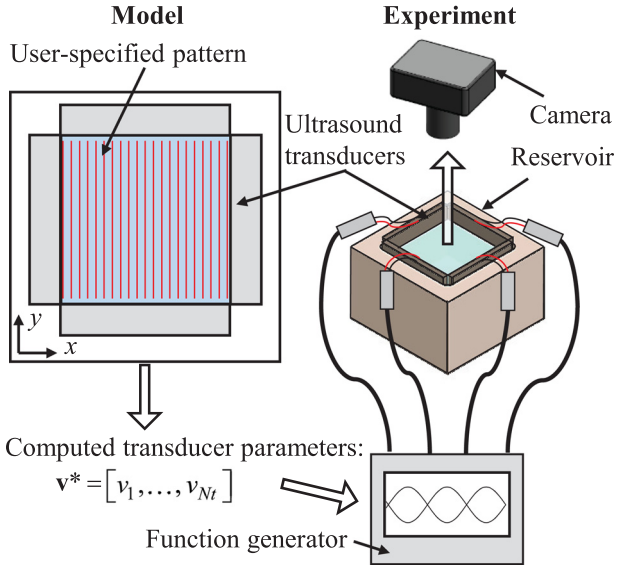

FIG. 3. Experimental validation of the inverse ultrasound directed self-assembly (DSA) method using a square reservoir filled with water and dispersed 80 nm carbon particles. A user-specified pattern is defined in the model and the ultrasound transducer parameters to obtain this pattern are computed using the inverse ultrasound DSA method (Eq. (10)). The ultrasound transducer parameters are then applied to the experimental set-up, assembling a pattern of nanoparticles, which is then compared to the user-specified pattern.

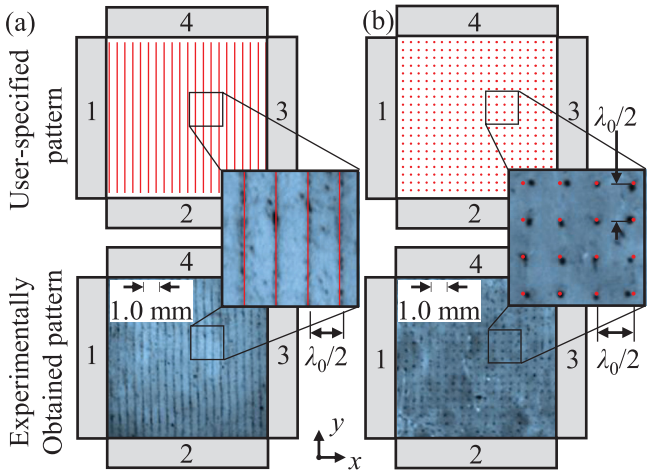

FIG. 4. User-specified patterns (red) and corresponding experimentally obtained patterns (black) assembled with the ultrasound transducer parameters calculated with the inverse ultrasound directed self-assembly method for a (a) line pattern, and (b) dot pattern of nanoparticles. Tables S I and S II list the ultrasound transducer parameters $\mathbf{v}^*$ to assemble the pattern of nanoparticles.[30]

Figure 4 shows two example patterns in a 12.75 $\times$ 12.75 mm square reservoir with $N_t = 4$. Feasible patterns for this ultrasound transducer arrangement include lines spaced $\lambda_0/2$ apart, parallel to a reservoir wall (Fig. 4(a)), and dots arranged in a square grid formation spaced $\lambda_0/2$ apart (Fig. 4(b)). Additionally, using a 24.75 $\times$ 24.75 mm square reservoir with $N_t = 8$ enables assembly of more complex patterns, such as a shifted line pattern (Fig. 5(a)), and a mixed line/dot pattern (Fig. 5(b)). Figures 4 and 5 show the user-specified pattern (red) and experimentally obtained pattern (black) assembled using the computed ultrasound transducer parameters. The insets show a magnified view of the user-specified pattern superimposed on the experimentally obtained patterns. Tables S I–S IV (see supplementary material[30]) list the calculated ultrasound transducer parameters $\mathbf{v}^*$, i.e., the amplitude and phase of the harmonic velocity of the ultrasound transducer surface, that correspond with the experiments shown in Figs. 4 and 5, respectively, showing that non-trivial ultrasound transducer parameters are required to assemble seemingly intuitive user-specified patterns of nanoparticles.

To quantify the accuracy of the experimentally obtained pattern of nanoparticles with respect to the user-specified pattern, we calculate the pattern error E_{pat} as the average distance between the centers of the user-specified and experimentally obtained pattern features (lines or dots), normalized by the nominal pattern spacing $\lambda_0/2$, for line and dot patterns shifted in the x- and y-direction. Fig. 6 shows the pattern error as a function of the normalized pattern shift distance $\Delta x/\lambda_0 \in [0, 1/2)$ for line (triangle marker) and dot (dot marker) patterns. Tables S V and S VI (see supplementary material[30]) list the calculated ultrasound transducer parameters $\mathbf{v}^*$. The pattern error E_{pat} is less than 16.0% and 16.5% for line and dot patterns, respectively, indicating good agreement between the user-specified and experimentally assembled patterns of nanoparticles. The pattern error results from slight misalignment of the ultrasound transducers within the handmade reservoir, and from the ultrasound transducers not performing as perfect piston sources, as assumed in the theoretical model. We also note that it is possible for the experimentally obtained pattern to contain additional pattern features, not part of the user-specified pattern. For instance, it is possible to assemble a user-specified dot pattern with spacing $\lambda_0/2$ by producing a line pattern that passes through the desired dot locations. In these instances, the pattern error is insufficient to account for the additional features, and a more complex scoring algorithm, such as a template matching method used in image processing, is desirable.[31]

We have derived a method of directly solving the inverse ultrasound DSA problem that relates a user-specified pattern of nanoparticles in a fluid medium contained in an arbitrary shaped reservoir to the operating parameters of any arrangement of ultrasound transducers, enabling ultrasound

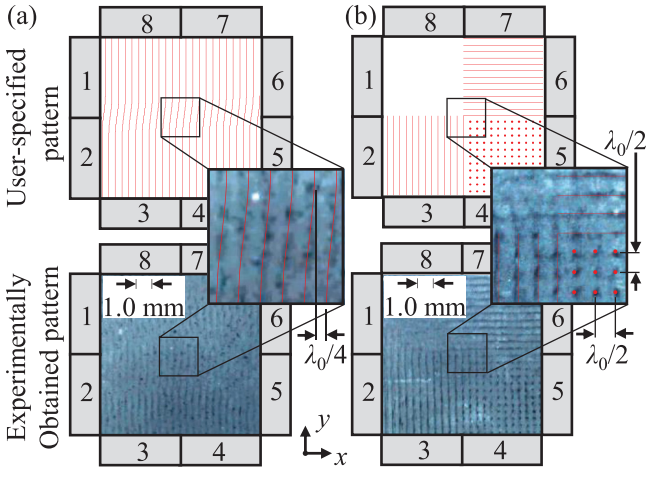

FIG. 5. User-specified patterns (red) and corresponding experimentally obtained patterns (black) assembled with the ultrasound transducer parameters calculated with the inverse ultrasound directed self-assembly method for a (a) shifted line pattern, and (b) mixed line/dot pattern of nanoparticles. Tables S III and S IV list the ultrasound transducer parameters $\mathbf{v}^*$ to assemble the pattern of nanoparticles.[30]

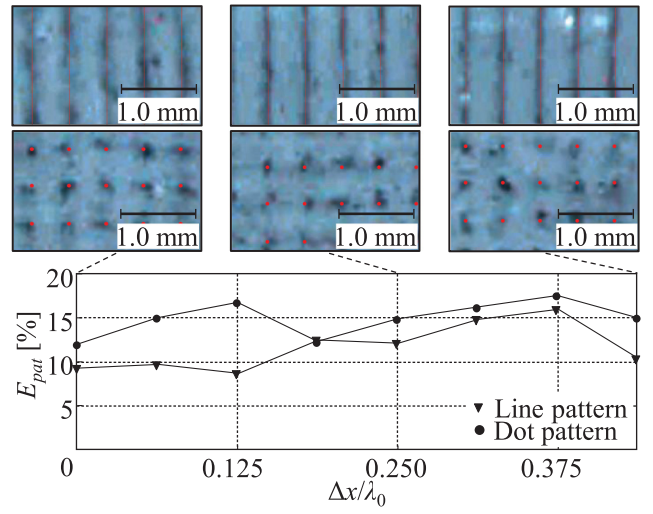

FIG. 6. Pattern error E_{pat} between experimentally obtained and user-specified line and dot patterns shifted in increments of $\Delta x/\lambda_0 = 0.0625$. Insets show images of the user-specified (red) and experimentally obtained (black) line and dot patterns for $\Delta x/\lambda_0 = \{0.000, 0.250, 0.438\}$. Tables S V and S VI list the ultrasound transducer parameters $\mathbf{v}^*$ to assemble the pattern of nanoparticles.[30]

DSA as a scalable fabrication technique. This work contrasts with existing indirect methods that require calculating complex maps of feasible patterns, and direct methods that only work for a limited set of reservoir and/or pattern geometries. In addition, the method accounts for all reflected waves, enabling experimental validation without requiring a complex setup with matching and backing layers to eliminate reflections. Thus, this method provides a practical approach of creating a user-specified pattern of nanoparticles using an arrangement of ultrasound transducers, in any reservoir geometry.

J.G. and B.R. acknowledge support from Army Research Office Contract# No. W911NF-14-1-0565 and National Aeronautics and Space Agency Award# No. NNX15AP30H. J.G. also acknowledges partial support of a NASA Space Technology Research Fellowship.

[1]M. Grzelczak, J. Vermant, E. M. Furst, and L. M. Liz-Marzán, ACS Nano **4**, 3591 (2010).
[2]Z. Nie, A. Petukhova, and E. Kumacheva, Nat. Nanotechnol. **5**, 15 (2010).
[3]S. B. Darling, Prog. Polym. Sci. **32**, 1152 (2007).
[4]Y. Chen, H. Liu, T. Ye, J. Kim, and C. Mao, J. Am. Chem. Soc. **129**, 8696 (2007).
[5]K. D. Hermanson, S. O. Lumsdon, J. P. Williams, E. W. Kaler, and O. D. Velev, Science **294**, 1082 (2001).
[6]J. H. E. Promislow and A. P. Gast, Langmuir **12**, 4095 (1996).
[7]B. Raeymaekers, C. Pantea, and D. N. Sinha, J. Appl. Phys. **109**, 014317 (2011).
[8]P. V. Kamat, K. G. Thomas, S. Barazzouk, G. Girishkumar, K. Vinodgopal, and D. Meisel, J. Am. Chem. Soc. **126**, 10757 (2004).
[9]M. Fujiwara, E. Oki, M. Hamada, Y. Tanimoto, I. Mukouda, and Y. Shimomura, J. Phys. Chem. A **105**, 4383 (2001).
[10]L. E. Kinsler, *Fundamentals of Acoustics* (John Wiley, New York, 2000), p. 210.
[11]M. Evander and J. Nilsson, Lab Chip **12**, 4667 (2012).
[12]Y. Yamakoshi, Y. Koitabashi, N. Nakajima, and T. Miwa, Jpn. J. Appl. Phys., Part 1 **45**, 4712 (2006).
[13]Y. Yamakoshi, N. Nakajima, and T. Miwa, Jpn. J. Appl. Phys., Part 1 **46**, 4847 (2007).
[14]J. N. Coleman, U. Khan, W. J. Blau, and Y. K. Gun'ko, Carbon **44**, 1624 (2006).
[15]V. M. Shalaev, Nat. Photonics **1**, 41 (2007).
[16]S. J. Corbitt, M. Francoeur, and B. Raeymaekers, J. Quant. Spectrosc. Radiat. Transfer **158**, 3 (2015).
[17]D. Haslam and B. Raeymaekers, Compos., Part B - Eng. **60**, 91 (2014).
[18]L. P. Gor'kov, Sov. Phys. - Dokl. **6**, 773 (1962).
[19]J. Greenhall, F. Guevara Vasquez, and B. Raeymaekers, Appl. Phys. Lett. **103**, 074103 (2013).
[20]T. Kozuka, K. Yasui, T. Tuziuti, A. Towata, and Y. Iida, Jpn. J. Appl. Phys., Part 1 **46**, 4948 (2007).
[21]A. Grinenko, C. K. Ong, C. R. P. Courtney, P. D. Wilcox, and B. W. Drinkwater, Appl. Phys. Lett. **101**, 233501 (2012).
[22]C. R. P. Courtney, B. W. Drinkwater, C. E. M. Demore, S. Cochran, A. Grinenko, and P. D. Wilcox, Appl. Phys. Lett. **102**, 123508 (2013).
[23]C. R. P. Courtney, C. E. M. Demore, H. Wu, A. Grinenko, P. D. Wilcox, S. Cochran, and B. W. Drinkwater, Appl. Phys. Lett. **104**, 154103 (2014).
[24]A. Marzo, S. A. Seah, B. W. Drinkwater, D. R. Sahoo, B. Long, and S. Subramanian, Nat. Commun. **6**, 8661 (2015).
[25]L. C. Wrobel, *The Boundary Element Method, Applications in Thermo-Fluids and Acoustics* (John Wiley & Sons, Hoboken, 2002).
[26]M. A. Gerzon, J. Audio Eng. Soc. **33**, 859 (1985).
[27]O. Kirkeby and P. A. Nelson, J. Acoust. Soc. Am. **94**(5), 2992 (1993).
[28]J. D. Maynard, E. G. Williams, and Y. Lee, J. Acoust. Soc. Am. **78**, 1395 (1985).
[29]B. N. Parlett, *The Symmetric Eigenvalue Problem* (Prentice-Hall, Inc., Upper Saddle River, 1998).
[30]See supplementary material at http://dx.doi.org/10.1063/1.4943634 for the ultrasound transducer parameters used to create Figs. 4–6.
[31]B. Roberto, *Template Matching Techniques in Computer Vision: Theory and Practice* (Wiley, Hoboken, 2009).